

# Antarctic temperature and global sea level closely coupled over the past five glacial cycles

E. J. Rohling<sup>1</sup>\*, K. Grant<sup>1</sup>, M. Bolshaw<sup>1</sup>, A. P. Roberts<sup>1</sup>, M. Siddall<sup>2</sup>†, Ch. Hemleben<sup>3</sup> and M. Kucera<sup>3</sup>

**Ice cores from Antarctica record temperature and atmospheric carbon dioxide variations over the past six glacial cycles<sup>1,2</sup>. Yet concomitant records of sea-level fluctuations—needed to reveal rates and magnitudes of ice-volume change that provide context to projections for the future<sup>3–9</sup>—remain elusive. Reconstructions indicate fast rates of sea-level rise up to 5 cm yr<sup>-1</sup> during glacial terminations<sup>10</sup>, and 1–2 cm yr<sup>-1</sup> during interglacials<sup>11,12</sup> and within the past glacial cycle<sup>13</sup>. However, little is known about the total long-term sea-level rise in equilibration to warming. Here we present a sea-level record for the past 520,000 years based on stable oxygen isotope analyses of planktonic foraminifera and bulk sediments from the Red Sea. Our record reveals a strong correlation on multi-millennial timescales between global sea level and Antarctic temperature<sup>1</sup>, which is related to global temperature<sup>6,7</sup>. On the basis of this correlation, we estimate sea level for the Middle Pliocene epoch (3.0–3.5 Myr ago)—a period with near-modern CO<sub>2</sub> levels—at 25 ± 5 m above present, which is validated by independent sea-level data<sup>6,14–16</sup>. Our results imply that even stabilization at today's CO<sub>2</sub> levels may cause sea-level rise over several millennia that by far exceeds existing long-term projections<sup>3</sup>.**

Comparing records of atmospheric CO<sub>2</sub> concentrations and temperature from Antarctic ice cores with reconstructions of global sea-level/ice-volume variability can help to quantify the natural (pre-anthropogenic) relationships between these parameters on long, millennial to orbital timescales. It remains uncertain whether such relationships from pre-anthropogenic times—when temperature (partially) led CO<sub>2</sub> change<sup>2,17,18</sup>—may be directly applied for projections into a CO<sub>2</sub>-led greenhouse future. Regardless, they do serve to illustrate the total ice-volume response to global temperature changes on multi-millennial timescales, over which all feedback mechanisms have played out (that is, when sea level has reached an equilibrium state). To evaluate whether climate models include all processes and feedbacks needed for long-term future ice-volume projections, their performance may be tested by comparison of hindcasts with the natural relationships observed in past data.

We present a new high-resolution sea-level record for the past 520 kyr, and compare it with a highly resolved record of past temperature<sup>1</sup>, a fundamental control on ice volume. The amount of warming can then be related to concomitant CO<sub>2</sub> increases on the basis of either the observed past relationship for the past several glacial cycles<sup>1,2</sup>, or model-based relationships for a variety of anthropogenic greenhouse scenarios<sup>3</sup>. We use a record of Antarctic temperature changes relative to the mean of the past 1,000 yr (hereafter,  $\Delta T_{AA}$ ), which derives in a virtually linear manner from stable hydrogen isotope data from the European Project for the Ice

Coring in Antarctica (EPICA) Dome C ice core<sup>1</sup> (see the Methods section and Supplementary Information, Part S1). Fluctuations in  $\Delta T_{AA}$  have been found to reflect global temperature variations with a mean twofold polar amplification factor<sup>6,7</sup>.

Our new composite sea-level record is based on a combination of previously published data from 533 stable oxygen isotope ( $\delta^{18}\text{O}$ ) analyses of the planktonic foraminifer *Globigerinoides ruber* (white) from cores GeoTü-KL11 and MD92-1017 (refs 11, 19–22), with a suite of 1564 new data points based on analyses of both *G. ruber* and bulk sediment from central Red Sea sediment core GeoTü-KL09 (19°57.6' N, 38°8.3' E, 814 m water depth; hereafter KL09) (see the Methods section). All records are presented on the EPICA Dome C 3 (EDC3) chronology<sup>23</sup> on the basis of graphic correlation with the  $\Delta T_{AA}$  record<sup>1</sup> (see the Methods section and Supplementary Information, Part S2) (Fig. 1).

Following transformation of each  $\delta^{18}\text{O}$  record into relative sea level (RSL; see the Methods section), all values were combined into one data set, and a three-point moving average (hereafter RSL\*) was determined (Fig. 1). This was done in two stages: first, it was carried out on all data; second, it was carried out after exclusion of the past interglacial (marine isotope stage 5e, MIS-5e) values from KL09 (Fig. 1). This removal was carried out because the MIS-5e values in KL09 were found to have a distinct, temporally limited, offset relative to other sea-level indicators for that time, which is not replicated in other Red Sea cores (Fig. 1, and ref. 11). We use RSL\* with these outliers excluded. Sensitivity tests demonstrate that this outlier removal does not substantially affect our conclusions, except for making them slightly more conservative (see Supplementary Fig. S10, Part S4). The overall reproducibility of long-term Red Sea RSL reconstructions (on the basis of different cores, carrier media, operators, protocols and analytical equipment) is illustrated by the distribution of residuals around RSL\* (Fig. 1c):  $1\sigma = 6.5\text{ m}$  ( $N = 2,052$ ), in agreement with the method's theoretical confidence limits<sup>19</sup>. Sea-level agreement between RSL\* and U-Th-dated coral and speleothem data from globally widespread locations<sup>19,24,25</sup> corroborates RSL\* as a measure of global sea-level fluctuations (see Fig. 1 and the discussion of sea-level positions below -100 m in Supplementary Information, Part S3).

Our 520,000-year RSL\* curve is compared with  $\Delta T_{AA}$  (ref. 1) in Fig. 1e. We focus on the long-term natural relationship between temperature and equilibrium sea level (that is, millennial to orbital scale; our correlation cannot be used to characterize relationships through rapid climate events, for which a more detailed chronology will be needed). We consider the derived long-term natural  $\Delta T_{AA}$ -RSL\* relationship within a context of the natural  $\Delta T_{AA}$ -[CO<sub>2</sub>] relationship observed in Antarctic ice-core data<sup>1,2</sup>, Pliocene (3.0–3.5 Myr) sea-level and [CO<sub>2</sub>] estimates<sup>6,14–16</sup>

<sup>1</sup>School of Ocean and Earth Science, National Oceanography Centre, University of Southampton, Southampton SO14 3ZH, UK, <sup>2</sup>Lamont-Doherty Earth Observatory, 61 Route 9W—PO Box 1000, Palisades, New York 10964-8000, USA, <sup>3</sup>Institute of Geosciences, University of Tübingen, Sigwartstrasse 10, 72076, Tübingen, Germany. †Present address: Department of Earth Science, University of Bristol, Will's Memorial Building, Queen's Road, Bristol BS8 1RJ, UK. \*e-mail: E.Rohling@noc.soton.ac.uk.

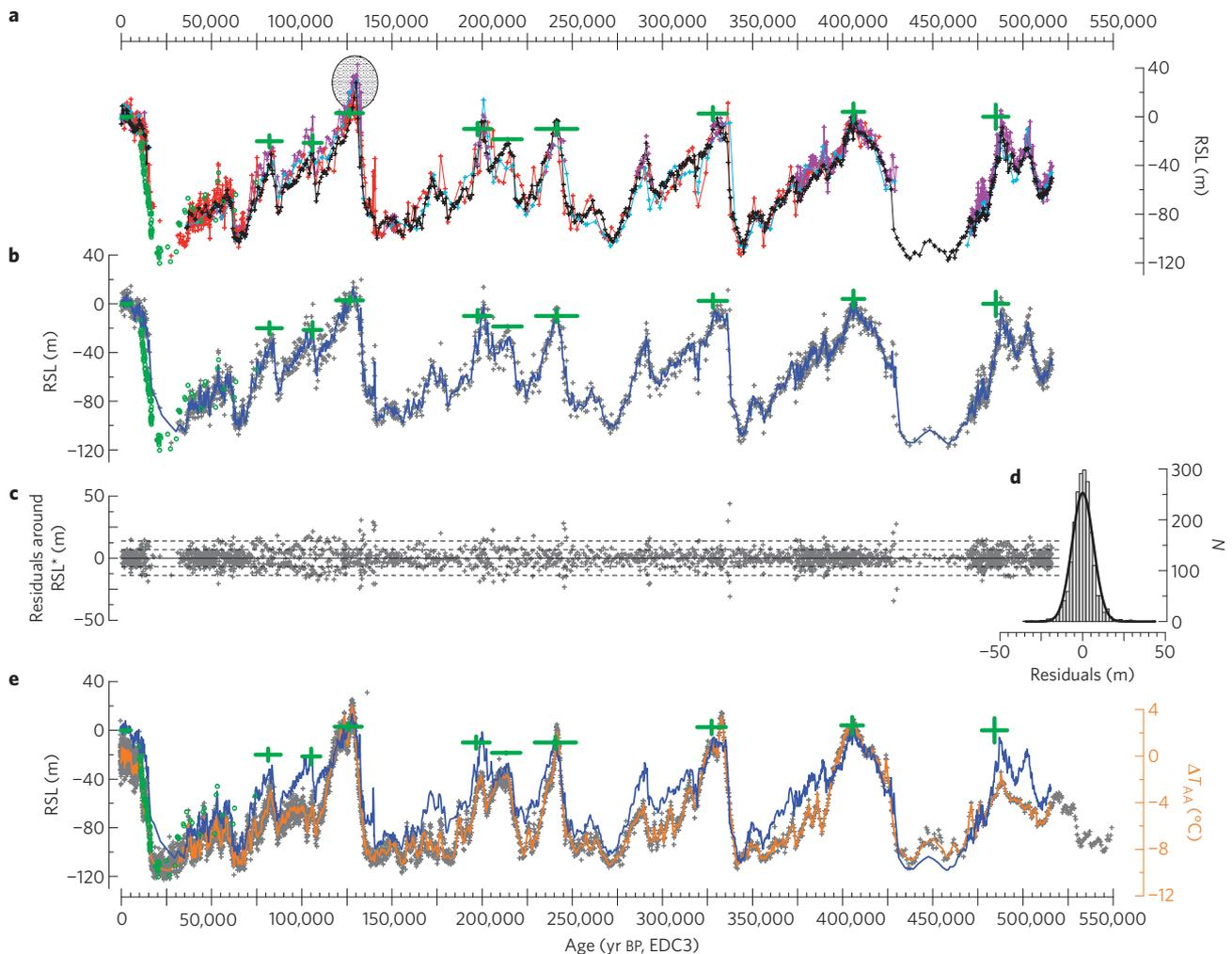


**Figure 1 | Composite Red Sea relative sea-level reconstruction (RSL\*), development and comparison with other data.** **a**, New RSL data from carbonate  $\delta^{18}\text{O}$  measurements on central Red Sea core GeoTü-KL09 (black: bulk sediment; purple: high-resolution *G. ruber*; light blue: pilot-sample<sup>26</sup> *G. ruber*), and previously published *G. ruber*-based data for nearby cores GeoTü-KL11 and MD92-1017 (red; refs 11, 19–22) (see the Methods section). The green symbols are coral and speleothem-based sea-level markers (also in **b** and **e**; refs 19, 24, 25) (all records on EDC3 (ref. 23) chronology; see the Methods section and Supplementary Information, Part S2). The shaded circle identifies outlier values for the past interglacial from core KLO9 (MIS-5e; see text). **b**, RSL\* (blue), determined as a three-point moving average through the combined central Red Sea RSL points from **a** (grey dots), after removal of outlier KLO9 MIS-5e values. **c**, Residuals around RSL\*, with  $\pm 1$  and  $2\sigma$  bands (dashed). **d**, Histogram of the residuals around RSL\*, with a Gaussian fit (heavy line) ( $N = 2,052$ ; mean = 0;  $1\sigma = 6.5$  m). **e**, Comparison of RSL\* (blue) and  $\Delta T_{AA}$  (ref. 1) (grey dots: all points; orange line: record subsampled at the same time-steps as RSL\*).

and model-based projections of the anthropogenically forced  $\Delta T_{AA}:[\text{CO}_2]$  relationship for the next century<sup>3</sup> (Fig. 2a).

Despite some differences, there is a striking overall similarity between RSL\* and  $\Delta T_{AA}$  (Fig. 1e). This long-term similarity over five complete glacial cycles echoes the previously noted similarity between Red Sea sea-level reconstructions and Antarctic climate proxies on millennial timescales<sup>13,19,21,26</sup> (see the Methods section and Supplementary Information, Part S2).

To enable quantitative comparison, the  $\Delta T_{AA}$  record was subsampled (linear interpolation between nearest neighbours) at the points where we have RSL\* values. Least-squares regression was carried out using a preferred exponential fit function (Supplementary Information, Part S3), which gives  $\text{RSL}^* = -47.716 \cdot e^{-0.110 \cdot \Delta T_{AA}} + 33.045$  (Fig. 2b). It has a coefficient of determination ( $\eta^2$ , equivalent to  $R^2$  in linear regressions) of 0.79 (see Supplementary Table S1, Part S4) and asymptotes to about +33 m at high  $\Delta T_{AA}$ . We show 95% confidence limits to the fit function (inner dashed lines) and to the data around the fit (outer dashed lines). The fit function is entirely and

uniquely determined by our new RSL\* data and  $\Delta T_{AA}$ . In validation, we plot the independent coral and speleothem-based points, as well as the Pliocene point with  $[\text{CO}_2]$  in the region of 360–20/+60 ppmv and global sea level 15–25 m above present<sup>6,14–16</sup>. The time span of the RSL\* reconstruction (~520 kyr) determines the temporal validity of our relationship, but the close fit with the Pliocene value suggests that the validity may extend to 3.5 Myr (Fig. 2b). Until it can be tested with older data, the relationship should be considered valid only back to—presumably Neogene—times during which (most of) the land-based East Antarctic ice sheet was in existence.

In Supplementary Information, Part S4, we investigate whether our  $\Delta T_{AA}:\text{RSL}^*$  relationship is statistically robust, using separate analyses of (parts of) the underlying raw component data sets (see Supplementary Fig. S8). We also test the inferred relationship with respect to two critical aspects: first, whether the relationship is the same or different when separately considering periods of rising and lowering sea level; and second, whether it is constant through time (Supplementary Information, Part S4). For the first

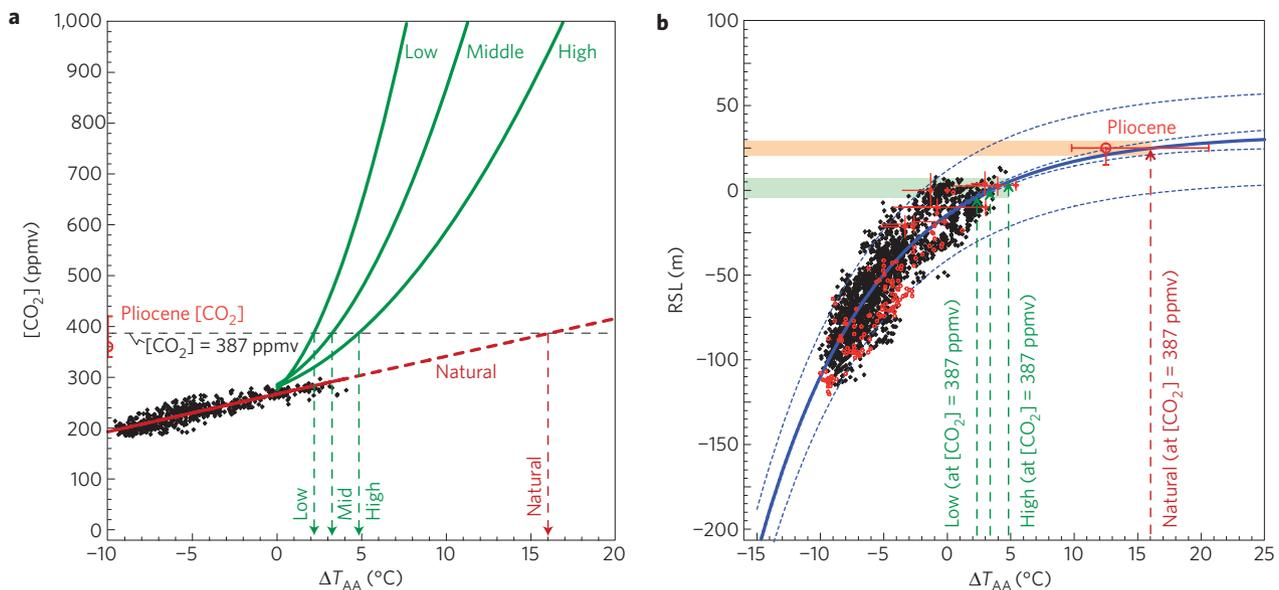


**Figure 2 | Temperature:RSL\* relationship and implications.** **a**, Natural (pre-anthropogenic)  $\Delta T_{AA}$ :[CO<sub>2</sub>] relationship from Antarctic ice-core data<sup>1,2</sup> (black dots, and red linear fit [CO<sub>2</sub>] = 7.43 $\Delta T_{AA}$  + 267.16 with  $R^2 = 0.8$ ), compared with Intergovernmental Panel on Climate Change model-summary equilibrium relationships for low, middle and high climate sensitivity<sup>3</sup> (green). The red circle with uncertainties represents the range of Middle Pliocene [CO<sub>2</sub>] estimates (see text; value positioned only on the CO<sub>2</sub> axis). The dashed black line indicates the (AD 2009) level of [CO<sub>2</sub>] = 387 ppmv, within Pliocene estimates. The arrows indicate  $\Delta T_{AA}$  values where [CO<sub>2</sub>] = 387 ppmv intersects the various  $\Delta T_{AA}$ :[CO<sub>2</sub>] relationships. **b**, Natural  $\Delta T_{AA}$ :RSL\* relationship for the past 520,000 years (this study; black dots). Validation from coral and speleothem-based data (see Fig. 1): small red dots for the past deglaciation, and larger red symbols for upper 2 $\sigma$  range estimates for past interglacials (these assume that peak sea-level coincided approximately with peak temperature). Also shown (red) is the Pliocene estimate, with sea level up to +25 m (see text). The solid blue line is the exponential fit function through the (black)  $\Delta T_{AA}$ :RSL\* data ( $N = 2,052$ ). The inner blue dashed lines are 95% confidence limits to the fit. The outer blue dashed lines are 95% confidence limits for data around the fit. The arrows and coloured bands give RSL implications of the  $\Delta T_{AA}$ :RSL\* relationship for [CO<sub>2</sub>] = 387 ppmv, in different scenarios from **a**.

test, we manually identified periods with clear rising and lowering sea-level trends in the RSL\* data set, and calculated separate least-squares exponential fits (see Supplementary Figs S8f and S9). The calculated fit functions are statistically indistinct from each other, and from the fit through all data points shown in Fig. 2b, at the 95% confidence level. This implies that the  $\Delta T_{AA}$ :RSL\* relationship remains fundamentally similar, regardless of whether the climate system is shifting towards glaciation or deglaciation; that is, there is no significant hysteresis in the  $\Delta T_{AA}$ :RSL\* relationship on the multi-millennial to orbital timescales considered. This data-driven observation corroborates modelling results that suggest only narrow hysteresis for trajectories that do not involve the main land-based East Antarctic ice sheet<sup>27</sup>. The second test considers whether our  $\Delta T_{AA}$ :RSL\* relationship is constant through time, by quantifying the distribution of residuals in the RSL\* data relative to RSL\* estimates projected from  $\Delta T_{AA}$  on the basis of our  $\Delta T_{AA}$ :RSL\* relationship (see Supplementary Fig. S11). This reveals an absence of systematic deviation (drift) from the inferred relationship throughout the past five glacial cycles. The various analyses in Supplementary Information, Part S4 illustrate that the fit function developed in Fig. 2b offers a robust description of this fundamental relationship in the climate system. This warrants its application to explore some key implications for the debate on potential future climate change.

The impacts of different scenarios of changing atmospheric CO<sub>2</sub> concentrations are illustrated together in Fig. 2a,b. The first scenario uses the natural  $\Delta T_{AA}$ :[CO<sub>2</sub>] relationship that is evident in Antarctic ice-core data<sup>1,2</sup> (Fig. 2a). Three further scenarios represent model-based equilibrium  $\Delta T_{AA}$ :[CO<sub>2</sub>] relationships based on runs with low, middle and high climate sensitivity<sup>3</sup> (accounting for a mean twofold polar temperature amplification factor<sup>6,7</sup>) (Fig. 2a).

In the first (natural) scenario, a rise in CO<sub>2</sub> levels from normal interglacial concentrations of 280 ppmv (ref. 2) to 387 ppmv (the modern level, which is within the range of Pliocene estimates) would lead to equilibrium ice-volume reduction towards a final state with sea level 25 ± 5 m above the present (again close to Pliocene values) (Fig. 2; Supplementary Table S1). Note that the industrial rate of CO<sub>2</sub> rise exceeds Quaternary rates by more than an order of magnitude, and that full equilibrium response/ice-volume adjustment requires multi-millennial timescales<sup>6</sup>. The three model-based scenarios<sup>3</sup> suggest that the  $\Delta T_{AA}$ :[CO<sub>2</sub>] relationship driven by anthropogenic emissions will differ considerably from the natural  $\Delta T_{AA}$ :[CO<sub>2</sub>] relationship observed in ice-core data (Fig. 2a). The lower projected  $\Delta T_{AA}$  increases (to 2–5 °C) in the model-based scenarios<sup>3</sup> lead to projected sea-level responses that are similarly smaller—they remain below a maximum of +5 m (Fig. 2b).

The various scenarios illustrated in Fig. 2 highlight an apparent discrepancy between model-based  $\Delta T_{AA}$ :[CO<sub>2</sub>] projections and the natural data (Fig. 2a). Partly, this may arise because the natural relationship may not stay linear with increasing [CO<sub>2</sub>], but change into an upward curve similar to the model results. As yet, however, this remains unconstrained. Another part of the discrepancy may be addressed from the observation that the high-climate-sensitivity model scenario comes closest to the natural  $\Delta T_{AA}$ :[CO<sub>2</sub>] relationship (Fig. 2a). The upper limit of climate sensitivity remains elusive<sup>28</sup>, and our results strongly corroborate previous suggestions that climate sensitivity may be considerably underestimated where equilibration over millennial timescales is concerned<sup>6,7,29</sup>. Finally, caution is needed when projecting the empirical natural relationships of Fig. 2 into the future, because they rely on natural (near-)equilibrium CO<sub>2</sub> values, whereas future projections need to account also for

ongoing emissions and feedback processes between warming and CO<sub>2</sub> release/uptake<sup>3,6,7</sup>.

Regardless of the uncertainties surrounding the use of any one of the specific scenarios in Fig. 2, it is clear that equilibrium sea level for the present-day [CO<sub>2</sub>] of 387 ppmv resides within a broad range between 0 and +25 (±5) m. The lower limit of that range derives from model projections<sup>3</sup>, whereas the upper limit derives from data describing the Earth system's pre-anthropogenic behaviour over the past 0.5–3.5 Myr (this study). Development of more accurate constraints will require climate models that are able to account for the key features of the pre-anthropogenic sea-level record. This is a critical research target, because the magnitude of the difference between actual and equilibrium sea level may affect the probability of rapid sea-level adjustment pulses. Past pulses of sea-level adjustment showed typical rates of 1.0–1.5 cm yr<sup>-1</sup> (refs 11–13, 19, 21, 22, 26) (including adjustments above the present-day level<sup>11</sup>), up to deglaciation extremes of 5 cm yr<sup>-1</sup> (ref. 10). Recent empirical/statistical studies suggest similarly high mean rates of sea-level rise for the next century (0.5–1.4 and 0.9–1.3 cm yr<sup>-1</sup>; refs 5, 8). Such rates are feasible from an ice-dynamical point of view<sup>9</sup>. Within that context, the inferred natural long-term CO<sub>2</sub>:ΔT<sub>AA</sub>:RSL\* relationships suggest that even long-term stabilization at the present-day CO<sub>2</sub> level may result in rising sea levels for the next two to five millennia, to a level up to 3–4 times higher than the existing long-term projection of +7 m (ref. 3).

## Methods

The new KL09 data comprise three sets of stable oxygen isotope (δ<sup>18</sup>O) analyses: first, 661 analyses of δ<sup>18</sup>O from 2 mg samples of dried, homogenized bulk sediment (δ<sup>18</sup>O<sub>bulk</sub>; average of 800 yr resolution); second, 169 δ<sup>18</sup>O analyses of non-size-constrained picks of the planktonic foraminiferal species *G. ruber* from an independently obtained set of pilot samples through the core that was initially intended only for stratigraphy (pilot δ<sup>18</sup>O<sub>ruber</sub>; ref. 26); and third, 734 carefully prepared δ<sup>18</sup>O analyses of 20–30 specimens of *G. ruber* (white) in a narrow (320–350 μm) size range, at high resolution (down to 150–300 yr) through key intervals of the core (high-resolution δ<sup>18</sup>O<sub>ruber</sub>). The various analyses are highly reproducible (Fig. 1), even though the carrier media are different and (virtually) independent, and the pilot-sample data represent an independent sampling of the core relative to the main data set. The high-resolution δ<sup>18</sup>O<sub>ruber</sub> analyses concern specific morphotypes of a particular planktonic foraminiferal species that lives in the uppermost 50 m of the water column, which are hand-picked from a narrow size window and hand-cleaned. The δ<sup>18</sup>O<sub>bulk</sub> analyses represent an indiscriminate mix of carbonate materials from planktonic and benthic foraminifera, nanofossils, pteropods, halimeda, inorganically precipitated carbonates and so on (CaCO<sub>3</sub> concentrations between 60 and 90%). That the δ<sup>18</sup>O of such vastly different carriers reveals the observed consistent variability (Fig. 1a) bears testimony to the common forcing of Red Sea δ<sup>18</sup>O, namely sea-level controlled changes in the residence-time of sea water in the basin<sup>19,30</sup>. Isostatic effects are accounted for in the RSL values calculated (see Supplementary Fig. S4, Part S1).

For 107 samples, both δ<sup>18</sup>O<sub>bulk</sub> and δ<sup>18</sup>O<sub>ruber</sub> were measured, which reveals a strong correlation (δ<sup>18</sup>O<sub>ruber</sub> = 0.93δ<sup>18</sup>O<sub>bulk</sub> - 2.30; R<sup>2</sup> = 0.9) (Supplementary Information, Part S1). This equation was used to translate δ<sup>18</sup>O<sub>bulk</sub> values into δ<sup>18</sup>O<sub>ruber</sub> equivalents. All KL09 records were then shifted so that their mean δ<sup>18</sup>O values for the past 6,000 years were equal to the mean δ<sup>18</sup>O<sub>ruber</sub> of the past 6,000 years in core GeoTü-KL11 (that is, -2.011‰), which formed the basis for our Red Sea sea-level calibration model<sup>19</sup>. Next, the records were translated into pre-uplift-correction RSL change using a polynomial approximation of the original Red Sea sea-level model<sup>19</sup> (Supplementary Information, Part S1). Finally, we applied a small strait uplift correction of 2 cm kyr<sup>-1</sup> (ref. 19), the need for which was first inferred from a long-term (glacial cycle scale) drift in salinity-dependent microfossil abundance and species composition within Red Sea sediment sequences, and comparison of Red Sea RSL data with independent RSL data<sup>20</sup>.

The KL09 data set has been placed on the EDC3 chronology using graphic correlation between the continuous δ<sup>18</sup>O<sub>bulk</sub> record and ΔT<sub>AA</sub> (ref. 1) to transform down-core depths to age (EDC3 timescale<sup>23</sup>) (see discussion in Supplementary Information, Part S2). The same was done for the KL11/MD92-1017 data set. Although most glacial-interglacial ice-volume variability was due to Northern Hemisphere ice sheets, comparison of the RSL data with ΔT<sub>AA</sub> is appropriate on the longer (orbital) timescales relevant to the present letter, because the EDC3 chronology of Antarctic climate records is in good agreement with the chronology of benthic isotope stacks that have a strong age dependence on orbital (June) insolation variations at 65° N latitude<sup>23</sup> (with a systematic millennial-scale offset, which we also recognize relative to U–Th-dated corals for the past deglaciation—see

below). Although less relevant to the issues studied here, this comparison seems to remain valid by approximation on shorter, millennial timescales<sup>13,19,21,26</sup> (see Supplementary Information, Part S2). We note that the EDC3 chronology differs in detail from the U–Th chronology of coral records for the past deglaciation, which seems roughly 2 kyr younger. When plotting U–Th-dated points in our EDC3-based graphs, we systematically shift the U–Th values by 2 kyr (to older positions), similar to the shift applied to benthic isotope data in the original EDC3 paper<sup>23</sup>. For the main glacial terminations, a lag of several kiloyears between Antarctic warming and ice-volume reduction makes sense given that ice volume probably responds to a millennial-scale period of integrated warming rather than instantaneous temperature (see extensive discussion in Supplementary Information, Part S2). When considering correlations between sea-level data and ΔT<sub>AA</sub>, we are therefore aware that sea-level change in real terms lags temperature change, but there is no technique available (yet) to resolve the magnitude of such a lag throughout the record (co-registered sea-level and climate proxies from a single Red Sea sample-set in the interval 65–45 kyr BP suggest that the signals at that time were coincident within the timing uncertainty that applies to methane synchronization of Greenland and Antarctic ice-core records<sup>26</sup>). In the absence of detailed timing constraints throughout the record, we use the optimum (lagged) correlation in a similar way as that used between CO<sub>2</sub> concentrations and hydrogen isotope ratios in Antarctic ice cores<sup>2</sup>.

Received 21 November 2008; accepted 27 May 2009;  
published online 21 June 2009

## References

- Jouzel, J. *et al.* Orbital and millennial Antarctic climate variability over the past 800,000 years. *Science* **317**, 793–796 (2007).
- Siegenthaler, U. *et al.* Stable carbon cycle-climate relationship during the Late Pleistocene. *Science* **310**, 1313–1317 (2005).
- Pachauri, R. K. & Reisinger, A. (eds) *Climate Change 2007 Synthesis Report—Contribution of Working Groups I, II and III to the Fourth Assessment Report of the Intergovernmental Panel on Climate Change* (IPCC, 2007); available at <http://www.ipcc.ch/ipccreports/ar4-syr.htm>.
- Alley, R. B., Clark, P. U., Huybrechts, P. & Joughin, I. Ice-sheet and sea-level changes. *Science* **310**, 456–460 (2005).
- Rahmstorf, S. A semi-empirical approach to projecting future sea-level rise. *Science* **315**, 368–370 (2007).
- Hansen, J. *et al.* Climate change and trace gases. *Phil. Trans. R. Soc. Lond. A* **365**, 1925–1954 (2007).
- Hansen, J. *et al.* Target atmospheric CO<sub>2</sub>: Where should humanity aim? *Open Atmos. Sci. J.* **2**, 217–231 (2008).
- Grinsted, A., Moore, J. C. & Jevrejeva, S. Reconstructing sea level from paleo and projected temperatures 200 to 2100 AD. *Clim. Dyn.* doi: 10.1007/s00382-008-0507-2 (2009).
- Pfeffer, W. T., Harper, J. T. & O'Neel, S. Kinematic constraints on glacier contributions to 21st-century sea-level rise. *Science* **321**, 1340–1343 (2008).
- Fairbanks, R. G. A 17,000 year glacio-eustatic sea level record: Influence of glacial melting rates on the Younger Dryas event and deep ocean circulation. *Nature* **342**, 637–642 (1989).
- Rohling, E. J. *et al.* High rates of sea-level rise during the last interglacial period. *Nature Geosci.* **1**, 38–42 (2008).
- Carlson, A. E. *et al.* Rapid early Holocene deglaciation of the Laurentide ice sheet. *Nature Geosci.* **1**, 620–624 (2008).
- Siddall, M., Rohling, E. J., Thompson, W. G. & Waelbroeck, C. Marine isotope stage 3 sea level fluctuations: Data synthesis and new outlook. *Rev. Geophys.* **46**, RG4003 (2008).
- Dowsett, H. J. *et al.* Joint investigations of the Middle Pliocene climate. *Glob. Planet. Change* **9**, 169–195 (1994).
- Royer, D. L. CO<sub>2</sub>-forced climate thresholds during the Phanerozoic. *Geochim. Cosmochim. Acta* **70**, 5665–5675 (2006).
- Naish, T. *et al.* Obliquity-paced Pliocene West Antarctic ice sheet oscillations. *Nature* **458**, 322–328 (2009).
- Ahn, J. & Brook, E. J. Atmospheric CO<sub>2</sub> and climate from 65 to 30 ka BP. *Geophys. Res. Lett.* **34**, L10703 (2007).
- Loulergue, L. *et al.* New constraints on the gas age-ice age difference along the EPICA ice cores, 0–50 kyr. *Clim. Past* **3**, 527–540 (2007).
- Siddall, M. *et al.* Sea-level fluctuations during the last glacial cycle. *Nature* **423**, 853–858 (2003).
- Rohling, E. J. *et al.* Magnitudes of sea-level lowstands of the past 500,000 years. *Nature* **394**, 162–165 (1998).
- Rohling, E. J., Marsh, R., Wells, N. C., Siddall, M. & Edwards, N. Similar melt-water contributions to glacial sea-level variability from Antarctic and northern ice sheets. *Nature* **430**, 1016–1021 (2004).
- Siddall, M., Bard, E., Rohling, E. J. & Hemleben, Ch. Sea-level reversal during Termination II. *Geology* **34**, 817–820 (2006).
- Parrenin, F. *et al.* The EDC3 chronology for the EPICA Dome C ice core. *Clim. Past* **3**, 485–497 (2007).

24. Siddall, M., Chappell, J. & Potter, E. K. in *The Climate of Past Interglacials* (eds Sirocko, F., Litt, T., Claussen, M. & Sanchez-Goni, M. F.) 75–92 (Elsevier, 2006).
25. Dutton, A. *et al.* Phasing and amplitude of sea-level and climate change during the penultimate interglacial. *Nature Geosci.* **2**, 355–359 (2009).
26. Rohling, E. J. *et al.* New constraints on the timing and amplitude of sea level fluctuations during early to middle marine isotope stage 3. *Paleoceanography* **23**, PA3219 (2008).
27. Pollard, D. & DeConto, R. M. Modelling West Antarctic ice sheet growth and collapse through the past five million years. *Nature* **458**, 329–332 (2009).
28. Knutti, R. & Hegerl, G. C. The equilibrium sensitivity of the Earth's temperature to radiation changes. *Nature Geosci.* **1**, 735–743 (2008).
29. Pagani, M., Caldeira, K., Archer, D. & Zachos, J. C. Atmosphere: An ancient carbon mystery. *Science* **314**, 1156–1157 (2006).
30. Biton, E., Gildor, H. & Peltier, W. R. Relative sea level reduction at the Red Sea during the Last Glacial Maximum. *Paleoceanography* **23**, PA1214 (2008).

## Acknowledgements

This study contributes to UK Natural Environment Research Council (NERC) project NE/C003152/1, the NERC Response of humans to abrupt environmental transitions consortium (RESET, NE/E01531X/1), and German Science Foundation (DFG) projects He 697/17; Ku 2259/3. M.S. acknowledges support from a fellowship at the Lamont Doherty Earth Observatory and an RCUK fellowship from the University of Bristol.

## Author contributions

All authors contributed extensively to the work presented in this letter.

## Additional information

Supplementary information accompanies this paper on [www.nature.com/naturegeoscience](http://www.nature.com/naturegeoscience). Reprints and permissions information is available online at <http://npg.nature.com/reprintsandpermissions>. Correspondence and requests for materials should be addressed to E.J.R.